Reconstruction of local magnetic properties of steel sheets by needle probe methods using space mapping techniques

G. Crevecoeur,[a] L. Dupre, and L. Vandenbossche
Department of Electrical Energy, Systems and Automation, Ghent University, Sint-Pietersnieuwstraat 41, B-9000 Gent, Belgium

R. Van de Walle
Department of Electronics and Information Systems, Ghent University, Sint-Pietersnieuwstraat 41, B-9000 Gent, Belgium

(Presented on 1 November 2005; published online 26 April 2006)

Cutting stresses introduced by punching influence the magnetic characteristics of electrical steels. A nondestructive experimental method used for measuring flux distributions in laminations is the needle probe method. The probe signals can be simulated by solving the two-dimensional nonlinear diffusion equation for the magnetic field in combination with a proper Preisach model. The Preisach parameters in several subregions of the steel sheet which best fit the input probe signals are obtained by solving the inverse problem. The method used for minimizing the cost function is the space mapping technique. This technique combines the fine model, which uses the finite element method, with a semianalytical coarse model, which reduces the nonlinear problem to a linear problem.
 [DOI: 10.1063/1.2176321]

I. INTRODUCTION

Stresses and strains due to manufacturing processes alter the global behavior of electrical machines. The local mechanical state, changed by the introduction of cutting stresses, influences the local magnetic properties of the material.[1] Due to the fact that these edge damages are mostly located in the vicinity of the critical parts of a device, the influence can become large. Therefore the need to determine the changes in the magnetic properties of steel sheets as a function of the distance from the cutting edge exists. Search coils and the needle probe method (NPM) (Fig. 1), which was proposed by Werner,[2] are existing experimental methods for the measurement of flux distributions in electrical steels. Yamaguchi *et al.*[3] and Senda *et al.*[4] presented a theoretical analysis of the NPM and the possible errors. Loisos and Moses[5] discussed the specific problems of air flux and compared the search coil method with the NPM. The nondestructive NPM is strongly preferable for local identification of magnetic properties. However, a drawback of the NPM concerns the inhomogeneous region near the lamination edge.[6] The NPM for identifying local properties near the lamination edge is only acceptable when interpreting correctly the needle probe signals. Therefore, in this paper the electromagnetic phenomena in the cross section of the steel sheet are described by a two-dimensional (2D) nonlinear diffusion equation for the magnetic field in combination with space dependent material parameters. To determine these parameters from the needle probe signals, the space mapping (SM) technique is used. The performance of the SM technique is investigated in the presence of noise in the needle signals.

II. SPACE MAPPING TECHNIQUES

Traditional direct optimization techniques such as the Nelder-Mead simplex (NMS) and simulated annealing may demand large computational efforts when solving inverse problems. The SM technique, reviewed in Ref. 7, wants to overcome this problem by aligning a coarse and a fine model. The fine model generates the needle probe signals $\mathbf{f}(\mathbf{x}_f)$ with $\mathbf{x}_f$ the fine model material parameters, while the coarse model gives rise to the needle signals $\mathbf{c}(\mathbf{x}_c)$ with $\mathbf{x}_c$ the coarse model material parameters to be identified. The cost function to be minimized by the SM is the quadratic deviation between the measured needle probe signals and the simulated ones. The SM technique combines the fast computations of the coarse model with the accuracy of the fine model by performing a so-called parameter extraction (PE), where $\mathbf{p}(\mathbf{x}_f)$ is obtained, which yields an approximation of $\mathbf{f}(\mathbf{x}_f)$ by $\mathbf{c}[\mathbf{p}(\mathbf{x}_f)]$.

The aggressive space mapping (ASM) technique employs quasi-Newton iterations $\mathbf{x}_f^{(k)}$ in conjunction with the classical Broyden formula.[8] Finally, the hybrid aggressive space mapping (HASM) enables switching between direct optimization and SM. For further details, see Ref. 9.

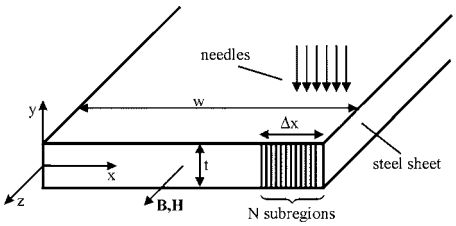

FIG. 1. Needle probe method.

[a]Electronic mail: guillaume.crevecoeur@ugent.be

III. FORWARD PROBLEM: COARSE AND FINE MODELS

In order to use SM techniques, a coarse and a fine model have to be available. Electromagnetic phenomena are described by the time and space variations of the magnetic field $\mathbf{H}=H(x,y,t)\mathbf{1}_z$ in a 2D cross section of the steel sheet as indicated in Fig. 1:

$$\frac{\partial^2 H}{\partial x^2}+\frac{\partial^2 H}{\partial y^2}=\sigma\frac{\partial B}{\partial H}\frac{\partial H}{\partial t}, \tag{1}$$

with the boundary condition $H_{\text{edge}}=H_0\sin(\omega t)$, describing the applied external field. The electrical conductivity is denoted by σ while $\partial B/\partial H$ describes the permeability. Hysteretic effects of magnetic materials can accurately be described by the commonly used Preisach theory.[10] Two Preisach models may be considered: (1) a scalar Preisach model with one input (the magnetic field) and one output (the magnetic induction), where the stress dependence can be incorporated through the Preisach distribution function (PDF), and (2) the vector Preisach model[11] with two inputs (the magnetic field and the stress) and two ouputs (the induction and the magnetostriction). Taking into account that $\mathbf{H}$ is unidirectional and that the magnetostriction is neglected in the model of the present paper, we consider the scalar model. The used Lorentzian expression for the PDF consists of an irreversible and a reversible part: $P(\alpha,\beta)=P_{\text{irr}}(\alpha,\beta)+P_{\text{rev}}(\alpha,\beta)$ with

$$P_{\text{irr}}(\alpha,\beta)=\frac{k_1}{[1+(\alpha-a)/b^2][1+(\beta+a)/b^2]}, \tag{2}$$

$$P_{\text{rev}}(\alpha,\beta)=\delta_{\alpha,\beta}\frac{k_2}{[1+(\alpha/c)^2]}. \tag{3}$$

$\delta_{\alpha,\beta}$ is the Kronecker delta symbol, α and β ($\beta\leqslant\alpha$) are the up and down switching fields, while a, b, c, k_1, and k_2 are fitting parameters. Due to the small thickness ($t\ll w$) of the sheet, we assume that the Preisach parameters are only a function of the x direction. Each subregion may have other values for a, b, c, k_1, and k_2. Once $H(x,y,t)$ is calculated, the eddy currents $\mathbf{J}=\text{curl}\,\mathbf{H}=\sigma\mathbf{E}$ can be determined in the cross section of the sheet. In particular, the probe signals on the surface can be quantified.

In the fine model, the local $H(x,y,t)$ values are calculated numerically using the finite element method.

In the coarse model, $H(x,y,t)$ values are evaluated in a semianalytical way as described below. The needle probe signals include two effects. The first effect, the edge effect, corresponds to the nonzero E_y component at the cutting edge of the sample, due to the ellipsoidal-type eddy currents. The second effect is due to nonuniform material characteristics.

In the coarse model we replace the hysteretic material by a linear, homogeneous medium with an average permeability given by

$$\mu_{\text{av}}=\frac{1}{2H_0}\int_{-H_0}^{H_0}d\alpha\int_{-H_0}^{\alpha}d\beta P(\alpha,\beta). \tag{4}$$

From the analytical solution $H(x,y,t)$ of the diffusion equation (1) with $\partial B/\partial H=\mu_{\text{av}}$,

$$H_0\frac{\sigma\mu_{\text{av}}}{4\pi t}\left\{\int_0^a[G(t,x-\xi,y)+G(t,x-\xi,y-t)]d\xi+\int_0^b[G(t,x,y-\eta)+G(t,x-w,y-\eta)]d\eta\right\}, \tag{5}$$

with $G(t,x-\xi,y-\eta)=(\sigma\mu_{\text{av}}/4\pi t)e^{-[(x-\xi)^2+(y-\eta)^2]\sigma\mu_{\text{av}}/4t}$, we obtain for the eddy currents $\underline{J}_x$ in the frequency domain, defining the probe signals,

$$\underline{J}_x(\omega,x,y)=\int_{-\infty}^{\infty}\frac{\partial H(x,y,t)}{\partial y}e^{-j\omega t}dt. \tag{6}$$

The integral (6) cannot be evaluated analytically, but is computed numerically by Fourier integrals using the discrete Fast fourier transform (FFT).

The nonhomogeneous properties of the material are incorporated by calculating (6) in a subregion with a certain μ_{av} as if this μ_{av} is the same everywhere else in the sample. It is obvious that this will introduce errors. In order to improve the alignment between the coarse and the fine model, we introduce in the coarse model hysteresis effects by substituting the average permeability in the diffusion equation with [12]

$$\mu_{\text{subst}}=\mu_{\text{av}}+\Delta\mu. \tag{7}$$

$\Delta\mu=\sqrt{(1/2H_0)\int_{-H_0}^{H_0}(\partial B/\partial H)^2dH-\mu_{\text{av}}^2}$ is the variation on the permeability.

IV. INVERSE PROBLEM

The Preisach parameters, which are functions of the distance from the cutting edge, are determined by solving the inverse problem. Here $5N$ Preisach parameters have to be fitted, with N the number of subregions with modified material parameters (a,b,c,k_1,k_2) considered at one cutting edge of the steel sheet. For the numerical experiments we took $t=0.1$ mm, $w=20$ mm, $\sigma=2.57\times10^6\ \Omega^{-1}$, N equal subregions with a total width of $\Delta x=10$ mm, and an applied field $H_0=100$ A/m with $\omega=2\pi50$ Hz. In order to have less parameters to be identified than the number of needles, we associate to each subregion with its set of Preisach parameters a mechanical state. This mechanical state is characterized by the stress σ_p. Then, measurements of a set of magnetization loops were carried out to determine the Preisach parameters as a function of σ_p, with σ_p having a range between 0 and 300 MPa. Consequently, it is possible to reduce the $5N$ Preisach unknowns to only N σ_p unknowns in the inverse problem.

Numerical experiments were carried out to investigate the accuracy and speed of the used algorithms. For a given $\boldsymbol{\sigma}_p^\star$ distribution, with $\boldsymbol{\sigma}_p^\star$ an N dimensional vector representing the σ_p in every subregion, the forward problem is solved with the numerical fine model, yielding a set of potentials $\mathbf{f}(\boldsymbol{\sigma}_p^\star)$. To these potentials Gaussian noise with a certain noise level nl is added. Hence we use white zero mean Gaussian noise with a standard deviation of $\mathcal{N}$. The noise level is defined as $nl=\mathcal{N}/V_{\text{rms}}$ with V_{rms} the root mean square of $\mathbf{f}(\boldsymbol{\sigma}_p^\star)$. The inverse problem was solved by finding the param-

TABLE I. Accuracy and CPU time without adding Gaussian noise in the numerical experiments.

ASM with	Accuracy	CPU time[a]
Coarse model using (4)	7.6	≈1 h
Coarse model using (7)	5.9	≈50 min
Numerical model with a coarse mesh	4.9	≈4 h
NMS method	1.0	≈8 h

[a]Time measure on a 2.4 GHz PC configuration.

eters $\bar{\boldsymbol{\sigma}}_p$ which best fit the noisy potentials after M iterations $\boldsymbol{\sigma}_p^{(l)}$, $l=1,\ldots,M$. The accuracy of the algorithms is defined as $\|\bar{\boldsymbol{\sigma}}_p-\boldsymbol{\sigma}_p^{\star}\|=\sqrt{\Sigma_{k=1}^{N}(\bar{\sigma}_{p,k}-\sigma_{p,k}^{\star})^2}$.

The most suitable direct optimization algorithm for minimizing in the fine model space is the nongradient based NMS method. Because this algorithm can easily be trapped in local minima and the global minimum can thus not be found, different start values for the algorithm are chosen. Up to 300 fine model evaluations are needed, corresponding to approximately 8 h of CPU time. If we do not make a reduction of parameters, then the computational cost becomes prohibitive. By implementing the ASM, less evaluations are needed in the fine model. The following three types of coarse models were separately implemented in the ASM algorithm: the coarse model using (4), the coarse model using (7), and the numerical model with a coarse mesh. Table I shows the accuracy and CPU time needed for solving one inverse problem. The values in this table and in the following figures are the average of the computation of 100 inverse problems with random $\boldsymbol{\sigma}_p^{\star}$ vectors. ASM with coarse model using (7) is a relatively accurate and very fast algorithm. This table shows that $\mathbf{c}(\mathbf{p})$ with $\mathbf{c}$ using (7) is a closer approximation to the fine model $\mathbf{f}$ than the coarse model without accounting the variation on the permeability.

The previous results can be explained mathematically if we place the SM formulation in the context of classical optimization methods. The so-called PE error $\bar{\varepsilon}=\|\mathbf{f}(\bar{\boldsymbol{\sigma}}_p)-\mathbf{c}(\mathbf{p}(\bar{\boldsymbol{\sigma}}_p))\|$ is an important measure for the convergence of the algorithm.[7] Figure 2 shows the drastic increase of the PE error as a function of noise level and shows that the numerical model with a coarse mesh generates smaller PE errors than the two other coarse models. The smaller $\bar{\varepsilon}$, the closer we approach the minimum and the more accurate the algorithm becomes.

Due to the fact that large variations of the magnetic

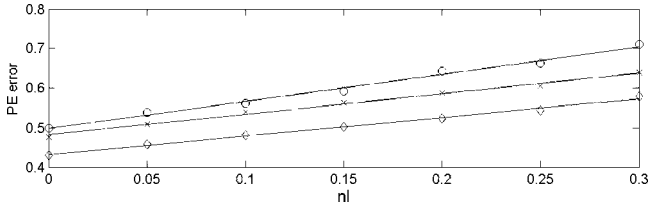

FIG. 2. PE error as a function of *nl*. "◇" is ASM with numerical model with a coarse mesh, "×" is ASM with coarse model using (7), and "○" is ASM with coarse model using (4).

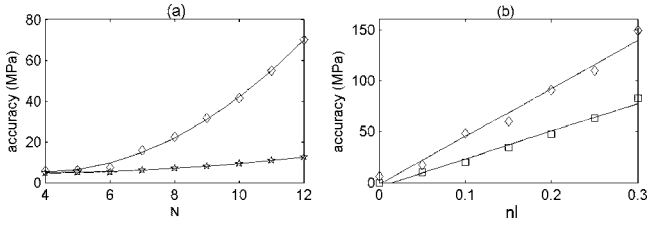

FIG. 3. Accuracy as a function of N (a) and accuracy as a function of nl (b). "◇" is ASM with coarse model using (7), "★" is ASM with fine model with a coarse mesh, and "□" is HASM with coarse model using (7).

properties may occur, a large number of parameters N will have to be fitted. Indeed, a larger N will give rise to a smoother function describing the variation of the magnetic properties. Because the number of needles is limited for practical reasons, N must be limited in order to keep a well conditioned inverse problem. $4\leqslant N\leqslant 12$ seems to be a good compromise. Figure 3(a) shows the accuracy as a function of the number of parameters to fit. The coarse model becomes relatively coarser to the fine one for increasing N, and simulates in a coarser way the nonhomogeneous magnetic properties. Nonlinearities in the fine model with coarse mesh will also appear in the fine model with fine mesh. A better mapping is thus constructed, which explains the figure.

If $\|\mathbf{f}(\boldsymbol{\sigma}_p^{(l)})-\mathbf{f}(\boldsymbol{\sigma}_p^{\star})\|$ is not going to zero, the ASM is not converging. Therefore we switch to direct optimization in the fine model (HASM). It is possible now to adjust the accuracy. For the same accuracy, the HASM using coarse model with (7) is on the average seen still eight times faster. The good robustness of the HASM to Gaussian noise is shown by Fig. 3(b).

V. CONCLUSION

Using SM techniques, we are able to identify the local magnetic parameters starting from the needle probe signals. The inverse problem is solved in an accurate, fast, and noise robust way by using, in particular, the HASM algorithm.

ACKNOWLEDGMENTS

This research was supported by the Special Research Fund (BOF) of the Ghent University.

[1]F. Ossart, E. Hug, O. Hubert, C. Buvat, and R. Billardon, IEEE Trans. Magn. **36**, 3137 (2000).
[2]E. Werner, Austrian Patent No. 191 015 (1949).
[3]T. Yamaguchi, K. Senda, M. Ishida, K. Sato, A. Honda, and T. Yamamoto, J. Phys. IV **8**, Pr2–717 (1998).
[4]K. Senda, M. Ishida, K. Sato, M. Komatsubara, and T. Yamaguchi, Electr. Eng. Jpn. **126**, 942 (1999).
[5]G. Loisos and A. Moses, IEEE Trans. Magn. **37**, 2755 (2001).
[6]H. Pfützner and G. Krismanic, IEEE Trans. Magn. **40**, 1610 (2004).
[7]J. Bandler, Q. Cheng, S. Dakroury, A. Mohamed, M. Bakr, K. Madsen, and J. Søndergaard, IEEE Trans. Microwave Theory Tech. **52**, 337 (2004).
[8]C. Broyden, Math. Comput. **19**, 577 (1965).
[9]M. Bakr, J. Bandler, N. Georgieva, and K. Madsen, IEEE Trans. Microwave Theory Tech. **47**, 2440 (1999).
[10]F. Preisach, Z. Phys. **94**, 277 (1935).
[11]A. Adly and I. Mayergoyz, IEEE Trans. Magn. **32**, 4773 (1996).
[12]B. Tellini, M. Bologna, and D. Pelliccia, IEEE Trans. Magn. **41**, 2 (2005).